

VIP Very Important Paper

Efficient Computation of Geometries for Gold Complexes

Isaac F. Leach,^[a, b] Leonardo Belpassi,^[c] Paola Belanzoni,^[c, d] Remco W. A. Havenith,^{*[a, b, e]} and Johannes E. M. N. Klein^{*[a]}

Computationally obtaining structural parameters along a reaction coordinate is commonly performed with Kohn-Sham density functional theory which generally provides a good balance between speed and accuracy. However, CPU times still range from inconvenient to prohibitive, depending on the size of the system under study. Herein, the tight binding GFN2-xTB method [C. Bannwarth, S. Ehlert, S. Grimme, *J. Chem. Theory Comput.* **2019**, *15*, 1652] is investigated as an alternative to produce reasonable geometries along a reaction path, that is,

reactant, product and transition state structures for a series of transformations involving gold complexes. A small mean error (1 kcal/mol) was found, with respect to an efficient composite hybrid-GGA exchange-correlation functional (PBEh-3c) paired with a double- ζ basis set, which is 2–3 orders of magnitude slower. The outlined protocol may serve as a rapid tool to probe the viability of proposed mechanistic pathways in the field of gold catalysis.

1. Introduction

Gold catalysis is a rapidly expanding field (for representative review articles see Ref. [1]) in which computational modelling is often used to aid the interpretation of experimental results. Typically, one would like to obtain a set of chemically-meaningful structures along a reaction path, to understand geometric and energetic changes. To this end, Kohn-Sham density functional theory (KS-DFT or simply DFT) is by far the most used method due to its favourable cost-accuracy ratio and applicability to a wide-range of organometallic systems.^[2] Particular exchange-correlation (XC) functional and basis set (BS) combinations (e.g. B3LYP/6-31G*)^[3] have found prolific use where

scalar relativistic effects are treated through the use of a pseudo potential (ECP).^[4] More recently, the ‘3c’ composite methods^[5] from the Grimme group have been put forward as a replacement as they overcome certain drawbacks.^[6] These methods reparameterize successful DFT functionals and introduce (empirical) contributions that efficiently correct for inherent limitations of the functional and small BS, such as corrections for the dispersion interaction^[7] and the (intra- and inter- molecular) basis set superposition error.^[8] These methods greatly facilitate computation of large systems. However, some calculations still require days of CPU time. Recently, an extremely fast semi-empirical tight binding method was proposed, coined GFN2-xTB^[9] and referred to hereafter as xTB.^[10] It seeks to approximate the KS-DFT energy in terms of fluctuations in the electron density and accounts for multipole electrostatics (up to 2nd order), (self-consistent) dispersion^[11] and static electron-electron correlation via Fermi smearing. xTB was parameterized for near-equilibrium geometries but has been shown to reproduce other equilibrium properties, such as dipole moments, better than all other semi-empirical approaches,^[9a] indicating the effectiveness of its parameterization strategy and physically-motivated design. If very large systems are to be treated the generally-applicable and robust GFN-FF force field is available.^[12] More recently, it was shown that xTB also produces good geometries for transition metal complexes.^[13] The article also alludes to applications of the xTB method for the study of reaction mechanisms which has previously been applied to, e.g. Zr complexes^[14] and lanthanoid complexes.^[15] While in the aforementioned studies, xTB is used to explore the reaction path, the transition states (TS) were still reoptimized with KS-DFT, which has recently been further explored in a semi-automated approach for organometallic complexes.^[16] With the field of gold chemistry and especially the area of catalysis in mind,^[1] a key question that arises from these reports is whether xTB can produce reasonable structures along a reaction path, including TS, for structures involving gold complexes. If so, it would be an effective tool to explore reactivity, especially for experimentalists who might only be interested in probing if a given


[a] I. F. Leach, Dr. R. W. A. Havenith, Dr. J. E. M. N. Klein
Molecular Inorganic Chemistry
Stratingh Institute for Chemistry
University of Groningen
9747 AG Groningen, The Netherlands
E-mail: r.w.a.havenith@rug.nl
j.e.m.n.klein@rug.nl


[b] I. F. Leach, Dr. R. W. A. Havenith
Zernike Institute for Advanced Materials
University of Groningen
9747 AG Groningen, The Netherlands

[c] Dr. L. Belpassi, Prof. Dr. P. Belanzoni
CNR Institute of Chemical Science and Technologies
“Giulio Natta” (CNR-SCITEC)
via Elce di Sotto 8, 06123 Perugia, Italy

[d] Prof. Dr. P. Belanzoni
Department of Chemistry, Biology and Biotechnology
University of Perugia
via Elce di Sotto 8, 06123 Perugia, Italy

[e] Dr. R. W. A. Havenith
Ghent Quantum Chemistry Group
Department of Inorganic and Physical Chemistry
Ghent University, 9000 Gent, Belgium

 Supporting information for this article is available on the WWW under <https://doi.org/10.1002/cphc.202001052>

 © 2021 The Authors. ChemPhysChem published by Wiley-VCH GmbH. This is an open access article under the terms of the Creative Commons Attribution Non-Commercial License, which permits use, distribution and reproduction in any medium, provided the original work is properly cited and is not used for commercial purposes.

scenario/path is viable or not, with the aim of supporting a mechanistic proposal rather than performing an extended computational study which would be much more time demanding and might be beyond the scope of a given study. In the present article we will demonstrate, for a series of transformations of gold complexes, that the xTB method provides meaningful structures that give insight into reaction mechanisms at very low computational cost. Some technical aspects are highlighted that make the use of the xTB method straightforward.

We begin by investigating the hydroamination of ethyne, shown in Figure 1, as a small model reaction following the procedure of Ciancaleoni *et al.*^[17] We compare xTB with a variety of the '3c' composite methods (HF-3c, PBEh-3c and B97-3c) and popular XC functional/basis set combinations combined with different dispersion correction schemes (B3LYP^[18]-D3(BJ)^[7,19]/def2-SVP,^[20] B3LYP^[18]-D3(BJ)^[7,19]/def2-TZVPP^[20] and B3LYP^[18]-D4^[11]/def2-TZVPP^[20]) for this purpose. These structures, and the additional tri-coordinated species (LAu(NH₃)(C₂H₂)), with geometries optimized at each of the stated methods define data set [A]. This allowed for an appropriate choice of DFT functional to compare xTB against in the second data set, [B], which consists of a representative set of stoichiometric gold reactions (shown in Figure 2), which generally include more realistically-sized systems. The geometries in data set [B] are optimized with PBEh-3c and xTB and include 1) the intramolecular oxidative addition of a naphthyl iodide moiety;^[21] 2) a Friedel-Crafts reaction with Au(I) & Au(III);^[22] 3) cyclopropanation involving a Au(I) carbene;^[23] 4) a 1,6-enyne cycloisomerization with Au(I)^[22] and 5) the gold-mediated Cope rearrangement of a 1,5-diene.^[24]

We probe the similarity of the xTB and PBEh-3c structures by evaluating their energies at the domain-based pair natural orbital coupled cluster method, DLPNO-CCSD(T),^[25] to provide a more accurate picture. We additionally use this opportunity to probe the accuracy of the double hybrid GGA XC functional B2-PLYP-D3(BJ) for the computation of accurate energetics of homogeneous gold systems, which has previously been shown to perform well for computational studies of gold chemistry.^[17,22,26] We also probe the Minnesota XC functional PW6B95-D3(BJ), which also performs well across all systems studied. Overall, the combination of xTB with the relatively inexpensive PW6B95-D3(BJ) functional (PW6B95-D3(BJ)//xTB)

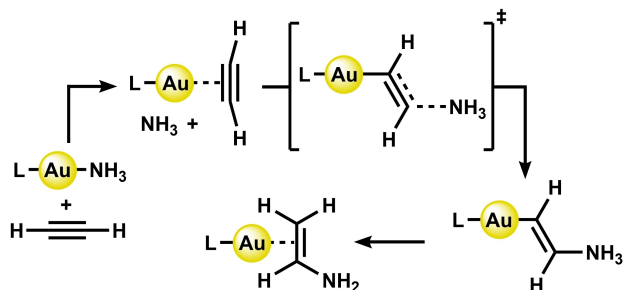
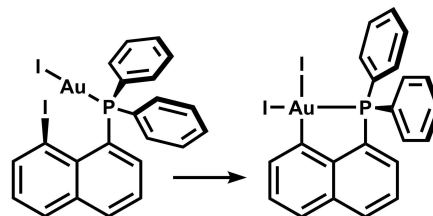
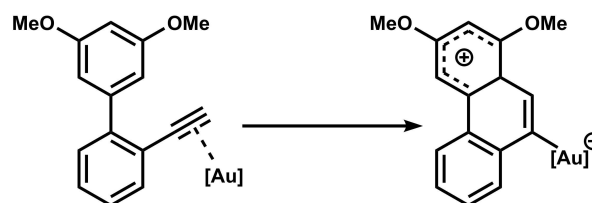


Figure 1. The stationary points along the reaction path of the hydroamination of data set [A], L=Cl,PH₃⁺.

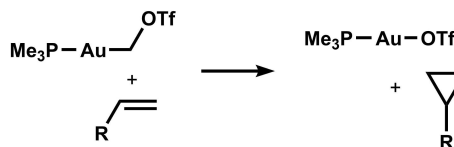
1) oxidative addition



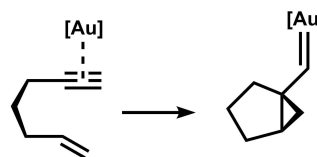
2) Friedel-Crafts reaction



3) cyclopropanation



4) cycloisomerization



5) Cope rearrangement

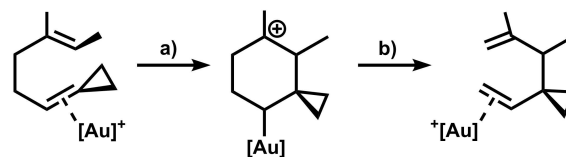


Figure 2. The small but diverse set of reactions selected for the main data set, [B], with larger Au complexes. [Au] = AuCl for reaction (2a), AuCl₃ for (2b), AuPH₃⁺ for (4) and AuPMe₃ for (5).

provides an excellent balance between rapid evaluation of geometries and accurate energetics.

Computational Details

General Comments

All calculations were performed with ORCA 4.2.1.^[27] xTB refers to GFN2-xTB v6.2.39^[28] and was used interfaced with ORCA. For xTB calculations the default SCF convergence criterion of 10^{-6} au was used. All other calculations use *VeryTightSCF* settings. The nature of all the stationary points was confirmed *via* frequency analyses and all TS structures were found to connect reactants and products *via* intrinsic reaction coordinate (IRC) calculations.^[29]

Hydroamination, Data Set [A]

All calculations were performed in the gas phase. The reference geometries were taken from Ciancaleoni *et al.*^[17] which had been computed at the density-fitting local coupled cluster (DF-LCCSD(T)/TZVPP) level of theory. In the present study these geometries were reoptimized with the selected methods shown below (Table 1).

For brevity, B3LYP-D3/S and B3LYP-D3/L are used throughout as labels to refer to B3LYP-D3(BJ)/def2-SVP and B3LYP-D3(BJ)/def2-TZVPP, respectively. Analytical second derivatives were used for KS-DFT calculations and HF-3c. For xTB calculations numerical second derivatives were employed. For all geometries, electronic energies were evaluated using the DLPNO-CCSD(T)^[32] level of theory in combination with the def2-TZVPP^[20] basis set and the def2-TZVPP/C^[33] fitting basis set. The *TightPNO* setting was used throughout.^[34] Relative electronic energies were compared, as outlined in ref. [17]. For KS-DFT, HF-3c and DLPNO-CCSD(T) calculations scalar relativistic effects were accounted for by replacing the 60 inner electrons of Au by the appropriate pseudo potential (ECP) for the specified basis set.^[4] DLPNO-CCSD(T)/def2-TZVPP single point energies obtained for the previously reported DF-LCCSD(T)/TZVPP geometries from ref. [17] are used as reference values.

Larger Au complexes, Data Set [B]

The performance of xTB and DFT (PBEh-3c) for structural parameters was further compared in data set [B]. For geometry optimizations with xTB the Generalized Born implicit solvation model with Surface Area contributions (GBSA, as implemented in the xTB code)^[28,35] with the default (230 point Lebedev) grid, was added, unless stated otherwise (see discussion below). To maintain consistency, the conductor-like polarizable continuum model (cPCM)^[32,36] was used for the corresponding PBEh-3c optimizations, using a modified (Gaussian van der Waals) cavity as implemented in ORCA.^[37] Water was specified in both cases. Numerical second derivatives were used for both DFT and xTB calculations. For *reaction 1* shown in Figure 2 we also computed nudged elastic band (NEB) paths^[38] (as implemented in the ORCA code)^[39] with various methods. Initial geometries for the five reactions were taken from refs. [21–24].

Table 1. Computational methods evaluated for data set [A].

Entry	Method	Basis Set
1	xTB ^[28]	–
2	HF-3c ^[30]	MINIX ^[30]
3	PBEh-3c ^[31]	def2-mSVP ^[31]
4	B97-3c ^[5a]	mTZVP ^[5a]
5	B3LYP ^[18] -D3(BJ) ^[7,19]	def2-SVP ^[20]
6	B3LYP ^[18] -D3(BJ) ^[7,19]	def2-TZVPP ^[20]

Final Single Point Energies

For comparison between the xTB and DFT geometries we again computed electronic energies at the DLPNO-CCSD(T)/def2-TZVPP level of theory as outlined above. In addition, we used this opportunity to probe the performance of the PW6B95 and B2-PLYP density functional approximations in combination with the D3(BJ) dispersion correction^[7] with Becke-Johnson damping^[19] (PW6B95-D3(BJ) and B2-PLYP-D3(BJ), respectively), employing the def2-TZVPP basis set. For these calculations *Grid6* and *GridX6* were used. Calculations were accelerated by the use of the *RIJCOSX* approximation^[40] using Weigend's universal fitting basis set.^[41] For B2-PLYP-D3(BJ), the *Rl* approximations was also employed for the MP2 step, using the def2-TZVPP/C fitting basis set.^[33] Energies were referenced to the fully separated reactants for the bimolecular cyclopropanation (3).

2. Results and Discussion

2.1. Hydroamination

The reliability of the calculated structural parameters of the various methods was judged by evaluating the energy of each structure with local coupled cluster DLPNO-CCSD(T)/def2-TZVPP. The errors were calculated as deviations with respect to the previously reported reference geometries.^[17] The statistics of these results can be found in Figure 3. xTB represents a clear improvement over HF-3c, despite being ~2 orders of magnitude faster. The other tested DFT functionals outperform xTB to a similar extent, with the exception of B3LYP-D3/L which produces the smallest errors (and has the largest basis set). The performance of the self-consistent D4 model was also probed and found to give quite comparable results to B3LYP-D3/L, indicating that the D3 dispersion correcting already performs very well. These results can be found in the Table S6. Despite this, PBEh-3c was selected for the more extensive comparison against xTB (data set [B]) as it is significantly more efficient than B3LYP-D3/L. This choice is further motivated by the common use of a hybrid GGA/double- ζ BS combination in computational

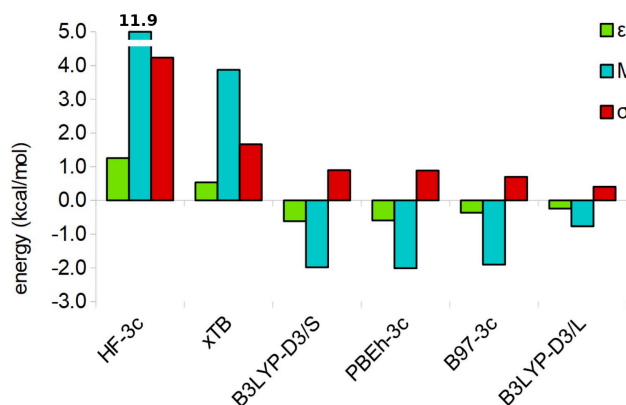


Figure 3. Mean Error (ϵ), Standard Deviation (σ) and Maximum Error (M) of the DLPNO-CCSD(T)/def2-TZVPP energy evaluated at the geometry of the tested methods, with respect to the previously reported^[17] DF-LCCSD(T) structures in data set [A].

respectively. The error statistics of this comparison can be found in Figure 6a and showcases xTB's good performance, with a low mean error ($\epsilon = -0.4$ kcal/mol) and standard deviation ($\sigma = 2.0$ kcal/mol). The Maximum Error ($M = -8.1$ kcal/mol) is due to the discussed difference in the cyclopropanated v_2 structures.

2.2.3. Structural Performance

The performance of xTB (vs. PBEh-3c) for obtaining structural parameters is examined explicitly in Table 2. The mean error of

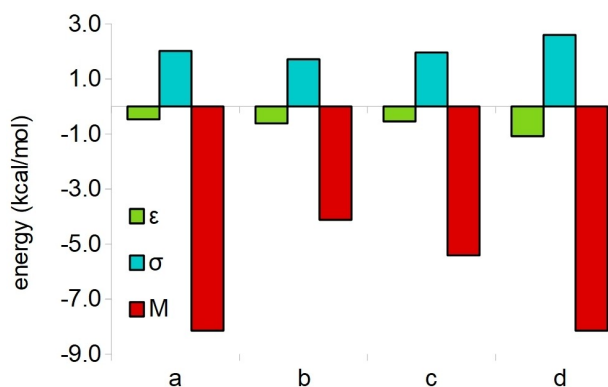


Figure 6. Mean Error (ϵ), Standard Deviation (σ) and Maximum Error (M) of a) DLPNO-CCSD(T)//xTB vs. DLPNO-CCSD(T)//PBEh-3c b) PW6B95-D3(BJ)//xTB vs. DLPNO-CCSD(T)//xTB c) B2-PLYP-D3(BJ)//xTB vs. DLPNO-CCSD(T)//xTB & d) PW6B95-D3(BJ)//xTB vs. DLPNO-CCSD(T)//PBEh-3c for data set [B].

the transition states ($\epsilon = -2.3$ pm) is marginally lower than that of the reactants and products (-2.9 & -3.0 pm, respectively), although there is a larger spread – seen in the greater standard deviation ($\sigma = 6.3$ pm vs. 3.1 & 3.2 pm) and maximum error ($M = -20.5$ pm vs. -10.3 & -11.1 pm).

2.2.4. Energetics

While DLPNO-CCSD(T) energies are feasible, they are far from convenient due to long CPU times and high memory usage. In practice, one would often like to acquire accurate energies with a less costly approach. Here, a small and non-exhaustive comparison is made between two such approaches: a DFT functional well-parameterized for thermodynamics (PW6B95-D3(BJ))^[44] and a double hybrid (B2-PLYP-D3(BJ))^[45] functional. Their deviations from the DLPNO-CCSD(T) reference for the data set [B] are shown in Figures 6b and 6c, respectively. Both methods perform similarly well, with PW6B95-D3(BJ)'s maximum error ($M = -4.1$ kcal/mol) a little lower than B2-PLYP-D3(BJ)'s ($M = -5.4$ kcal/mol). Notably, the maximum error corresponds in both cases to the transition state of reaction 1. Comparing PW6B95-D3(BJ) and PW6B95-D4 (i.e. replacing the D3 dispersion model with self-consistent D4 model)^[11] slightly reduced the standard deviation (σ) at no additional computational cost. These results, along with those of B3LYP-D3(BJ) can be found in the SI.

Since Figure 5 shows the good performance of xTB (vs. DFT) for structural parameters and Figure 6b shows the good

Table 2. Metal-to-ligand interatomic distances and error statistics (in pm) of the xTB optimized structures in data set [B],^[a] DFT refers to the composite PBEh-3c method.^[31]

Reaction	atom #1-atom #2 ^[b]	xTB			Deviation (w.r.t DFT)		
		R	TS	P	R	TS	P
1	Au-P ₄₀	226.7	247.6	226.0	-3.6	8.5	-5.3
	Au-I ₄₂	262.6	268.6		-1.6	-3.5	-3.3
	Au-I ₁₆	279.6	263.9		-1.5	-20.5	-4.7
	Au-C ₂	209.0	205.8		-0.2	-5.1	-1.6
2a	Au-Cl ₂₄	230.4	236.5		-10.3	-0.9	1.5
	Au-C ₂₀	205.0	202.5		-1.4	-0.7	0.3
	Au-C ₂₁	257.0	293.1		-4.9	-2.6	-0.3
2b	Au-Cl ₂₄	230.7	227.2		-2.4	0.9	-3.5
	Au-Cl ₂₅	230.6	240.5		-1.4	0.2	0.3
	Au-Cl ₂₆	231.0	227.3		-2.0	1.0	-3.2
	Au-C ₂₀	221.3	198.8		0.3	6.3	-2.5
4	Au-C ₂₁	237.2	288.4		-0.3	-7.7	-0.8
	Au-C ₂	283.0	305.1		1.8	4.5	-2.0
	Au-C ₃	208.9	202.0		-5.1	-0.4	-0.8
	Au-P ₁₁	228.5	229.0		-1.7	-2.7	-5.3
5	Au-P ₅	TS-I	int	R	TS-I	int	
	Au-C ₁	285.7	306.6		-5.7	-5.6	-3.8
	Au-O ₂₀	215.7	212.2		-9.1	-0.2	0.0
	Au-P ₂	227.8	228.6		-2.9	-3.1	-4.2
	Au-O ₁₆	TS-II	P		TS-II	P	
		216.0	230.4		0.0	-11.1	
		264.0	218.8		-14.2	-10.2	
		231.6	230.5		-3.2	-1.9	
Mean error (ϵ)					-2.9	-2.3	-3.0
Standard deviation (σ)					3.1	6.3	3.2
Maximum error (M)					-10.3	-20.5	-11.1

[a] The cyclopropanation (3) has been omitted due to the previously discussed qualitative differences, please see Table S8 for further information. [b] The subscripts in the atom labels correspond to the atom numbers in the xyz coordinate tables, which can be found in the Supporting Information.

performance of PW6B95-D3(BJ) (vs. DLPNO-CCSD(T)) for obtaining electronic energies, one may naturally ask if they might work together in a hybrid procedure of geometry optimization with xTB and single point energy evaluation with PW6B95-D3(BJ) (PW6B95-D3(BJ)//xTB). The error statistics of such an approach, with reference to the DLPNO-CCSD(T) energies evaluated at the DFT geometries (DLPNO-CCSD(T)//PBEh-3c), can be found in Figure 6d and demonstrate that the relative energies for all the species in Figure 2 (and the TS connecting them) could have been obtained, on average, within 1.1 kcal/mol at a mere fraction of the computational effort. The large maximum error ($M = -8.1$ kcal/mol) is due to the previously discussed complications of the cyclopropanation (Figure 5), which might be judged to be of limited relevance for exploring reaction paths.

3. Conclusions

The extremely efficient tight-binding method xTB was found to be capable of producing very reasonable geometries of five diverse reactions of Au complexes, in comparison to the well-balanced KS-DFT composite method PBEh-3c. This holds for both minima (as xTB was designed to do) and transition state geometries (a far-from equilibrium property that it was not originally intended for). PW6B95-D3(BJ) and B2-PLYP-D3(BJ) reproduced the DLPNO-CCSD(T) energies with similar accuracy. This is in line with the results of Dohm *et al.*,^[46] and demonstrate that well-parameterized (meta-)hybrid and double-hybrid density functionals can be effectively used to evaluate energies. The inclusion of an implicit solvation model for xTB optimizations was found to aid in reproducing DFT-like potential energy surfaces. Some care should be taken when examining ion pair/loosely bound complexes of bimolecular reactions as the only tested structure of this kind was found to be qualitatively different to DFT but aside from these caveats, PW6B95-D3(BJ)//xTB has been shown to be an effective tool at rapidly exploring the reactive space of Au complexes. Similarly, it has recently been shown that the conformational space of transition metal complexes may be efficiently probed with a similar computational procedure employing geometries from xTB,^[47] rendering this approach a comprehensive tool for the exploration of the chemical space of transition metal complexes. With the often more qualitative perspective of many experimental studies, asking simply if a proposed mechanistic pathway is feasible or not, we feel that xTB provides an excellent balance between speed and accuracy, especially when used in the proposed PW6B95-D3(BJ)//xTB scheme.

Acknowledgements

The authors would like to thank the Center for Information Technology of the University of Groningen for their support and for providing access to the Peregrine high-performance computing cluster. I.F.L. wishes to thank the Theoretical Chemistry group at the University of Groningen for its funding of his TCCM MSC.

J.E.M.N.K. acknowledges funding from the Netherlands Organisation for Scientific Research (NWO START-UP grant).

Conflict of Interest

The authors declare no conflict of interest.

Keywords: computational chemistry · geometries · gold catalysis · mechanistic pathways · xTB

- [1] a) L.-P. Liu, G. B. Hammond, *Chem. Soc. Rev.* **2012**, *41*, 3129–3139; b) I. Braun, A. M. Asiri, A. S. K. Hashmi, *ACS Catal.* **2013**, *3*, 1902–1907; c) H. Ohno, *Isr. J. Chem.* **2013**, *53*, 869–882; d) L. Zhang, *Acc. Chem. Res.* **2014**, *47*, 877–888; e) R. Dorel, A. M. Echavarren, *Chem. Rev.* **2015**, *115*, 9028–9072; f) D. Pflästerer, A. S. K. Hashmi, *Chem. Soc. Rev.* **2016**, *45*, 1331–1367; g) M. Zidan, S. Rohe, T. McCallum, L. Barriault, *Catal. Sci. Technol.* **2018**, *8*, 6019–6028.
- [2] a) L. Perrin, K. J. T. Carr, D. McKay, C. L. McMullin, S. A. Macgregor, O. Eisenstein, in *Struct. Bond.*, Springer International Publishing, **2015**, pp. 1–37; b) H. Ryu, J. Park, H. K. Kim, J. Y. Park, S.-T. Kim, M.-H. Baik, *Organometallics* **2018**, *37*, 3228–3239; c) X. Yang, T. Strassner, *J. Organomet. Chem.* **2018**, *864*, 1–168.
- [3] A. D. Becke, *J. Chem. Phys.* **1993**, *98*, 5648–5652.
- [4] D. Andrae, U. Häußermann, M. Dolg, H. Stoll, H. Preuß, *Theor. Chim. Acta* **1990**, *77*, 123–141.
- [5] a) J. G. Brandenburg, C. Bannwarth, A. Hansen, S. Grimme, *J. Chem. Phys.* **2018**, *148*, 064104; b) S. Grimme, J. G. Brandenburg, C. Bannwarth, A. Hansen, *J. Chem. Phys.* **2015**, *143*, 054107; c) R. Sure, S. Grimme, *J. Comput. Chem.* **2013**, *34*, 1672–1685.
- [6] H. Kruse, L. Goerigk, S. Grimme, *J. Org. Chem.* **2012**, *77*, 10824–10834.
- [7] S. Grimme, J. Antony, S. Ehrlich, H. Krieg, *J. Chem. Phys.* **2010**, *132*, 154104.
- [8] H. Kruse, S. Grimme, *J. Chem. Phys.* **2012**, *136*, 154101.
- [9] a) C. Bannwarth, S. Ehlert, S. Grimme, *J. Chem. Theory Comput.* **2019**, *15*, 1652–1671; b) S. Grimme, C. Bannwarth, P. Shushkov, *J. Chem. Theory Comput.* **2017**, *13*, 1989–2009.
- [10] C. Bannwarth, S. Ehlert, S. Grimme, *J. Chem. Theory Comput.* **2019**, *15*, 1652–1671.
- [11] E. Caldeweyher, S. Ehlert, A. Hansen, H. Neugebauer, S. Spicher, C. Bannwarth, S. Grimme, *J. Chem. Phys.* **2019**, *150*, 154122.
- [12] S. Spicher, S. Grimme, *Angew. Chem. Int. Ed.* **2020**, *59*, 15665–15673; *Angew. Chem.* **2020**, *132*, 15795–15803.
- [13] M. Bursch, H. Neugebauer, S. Grimme, *Angew. Chem. Int. Ed.* **2019**, *58*, 11078–11087; *Angew. Chem.* **2019**, *131*, 11195–11204.
- [14] Z. Jian, G. Kehr, C. G. Daniliuc, B. Wibbeling, T. Wiegand, M. Siedow, H. Eckert, M. Bursch, S. Grimme, G. Erker, *J. Am. Chem. Soc.* **2017**, *139*, 6474–6483.
- [15] M. Bursch, A. Hansen, S. Grimme, *Inorg. Chem.* **2017**, *56*, 12485–12491.
- [16] S. Dohm, M. Bursch, A. Hansen, S. Grimme, *J. Chem. Theory Comput.* **2020**, *16*, 2002–2012.
- [17] G. Ciancaleoni, S. Rampino, D. Zuccaccia, F. Tarantelli, P. Belanzoni, L. Belpassi, *J. Chem. Theory Comput.* **2014**, *10*, 1021–1034.
- [18] a) A. D. Becke, *Phys. Rev. A* **1988**, *38*, 3098–3100; b) C. Lee, W. Yang, R. G. Parr, *Phys. Rev. B* **1988**, *37*, 785–789; c) A. D. Becke, *J. Chem. Phys.* **1993**, *98*, 5648–5652.
- [19] S. Grimme, S. Ehrlich, L. Goerigk, *J. Comput. Chem.* **2011**, *32*, 1456–1465.
- [20] F. Weigend, R. Ahlrichs, *Phys. Chem. Chem. Phys.* **2005**, *7*, 3297–3305.
- [21] J. Guenr, S. Mallet-Ladeira, L. Estevez, K. Miqueu, A. Amgoune, D. Bourissou, *J. Am. Chem. Soc.* **2014**, *136*, 1778–1781.
- [22] R. Kang, W. Lai, J. Yao, S. Shaik, H. Chen, *J. Chem. Theory Comput.* **2012**, *8*, 3119–3127.
- [23] J. M. Sarria Toro, C. García-Morales, M. Raducan, E. S. Smirnova, A. M. Echavarren, *Angew. Chem. Int. Ed.* **2017**, *56*, 1859–1863; *Angew. Chem.* **2017**, *129*, 1885–1889.
- [24] R. J. Felix, D. Weber, O. Gutierrez, D. J. Tantillo, M. R. Gagné, *Nat. Chem.* **2012**, *4*, 405–409.
- [25] C. Riplinger, B. Sandhoefer, A. Hansen, F. Neese, *J. Chem. Phys.* **2013**, *139*, 134101.

- [26] R. Kang, H. Chen, J. Yao, S. Shaik, *J. Chem. Theory Comput.* **2011**, *7*, 4002–4011.
- [27] a) F. Neese, *WIREs Comput. Mol. Sci.* **2012**, *2*, 73–78; b) F. Neese, *WIREs Comput. Mol. Sci.* **2018**, *8*, e1327.
- [28] C. Bannwarth, S. Ehlert, S. Grimme, *J. Chem. Theory Comput.* **2019**, *15*, 1652–1671.
- [29] K. Ishida, K. Morokuma, A. Komornicki, *J. Chem. Phys.* **1977**, *66*, 2153–2156.
- [30] R. Sure, S. Grimme, *J. Comput. Chem.* **2013**, *34*, 1672–1685.
- [31] S. Grimme, J. G. Brandenburg, C. Bannwarth, A. Hansen, *J. Chem. Phys.* **2015**, *143*, 054107.
- [32] D. G. Liakos, M. Sparta, M. K. Kesharwani, J. M. L. Martin, F. Neese, *J. Chem. Theory Comput.* **2015**, *11*, 1525–1539.
- [33] A. Hellweg, C. Hättig, S. Höfener, W. Klopper, *Theor. Chem. Acc.* **2007**, *117*, 587–597.
- [34] D. G. Liakos, M. Sparta, M. K. Kesharwani, J. M. L. Martin, F. Neese, *J. Chem. Theory Comput.* **2015**, *11*, 1525–1539.
- [35] S. Grimme, C. Bannwarth, P. Shushkov, *J. Chem. Theory Comput.* **2017**, *13*, 1989–2009.
- [36] M. Cossi, N. Rega, G. Scalmani, V. Barone, *J. Comput. Chem.* **2003**, *24*, 669–681.
- [37] A. W. Lange, J. M. Herbert, *J. Chem. Phys.* **2010**, *133*, 244111.
- [38] a) H. Jónsson, G. Mills, K. W. Jacobson, in *Classical and Quantum Dynamics in Condensed Phase Simulations*, pp. 385–404; b) G. Mills, H. Jónsson, *Phys. Rev. Lett.* **1994**, *72*, 1124–1127; c) G. Mills, H. Jónsson, G. K. Schenter, *Surf. Sci.* **1995**, *324*, 305–337; d) G. Mills, H. Jónsson, G. K. Schenter, *Surf. Sci.* **1995**, *324*, 305–337.
- [39] a) F. Neese, *WIREs Comput. Mol. Sci.* **2012**, *2*, 73–78; b) F. Neese, *WIREs Comput. Mol. Sci.* **2018**, *8*, e1327; c) Asgeirsson, Birgirsson, Björnsson, Becker, Riplinger, Neese, Jonsson, (*In prep.*).
- [40] F. Neese, F. Wennmohs, A. Hansen, U. Becker, *Chem. Phys.* **2009**, *356*, 98–109.
- [41] F. Weigend, *Phys. Chem. Chem. Phys.* **2006**, *8*, 1057.
- [42] C. García-Morales, X.-L. Pei, J. M. Sarria Toro, A. M. Echavarren, *Angew. Chem. Int. Ed.* **2019**, *58*, 3957–3961; *Angew. Chem.* **2019**, *131*, 3997–4001.
- [43] a) J. E. M. N. Klein, G. Knizia, L. Nunes dos Santos Comprido, J. Kästner, A. S. K. Hashmi, *Chem. Eur. J.* **2017**, *23*, 16097–16103; b) L. Nunes dos Santos Comprido, J. E. M. N. Klein, G. Knizia, J. Kästner, A. S. K. Hashmi, *Chem. Eur. J.* **2016**, *22*, 2892–2895; c) R. Hahn, F. Bohle, W. Fang, A. Walther, S. Grimme, B. Esser, *J. Am. Chem. Soc.* **2018**, *140*, 17932–17944; d) R. Hahn, F. Bohle, S. Kotte, T. J. Keller, S.-S. Jester, A. Hansen, S. Grimme, B. Esser, *Chem. Sci.* **2018**, *9*, 3477–3483.
- [44] Y. Zhao, D. G. Truhlar, *J. Phys. Chem. A* **2005**, *109*, 5656–5667.
- [45] S. Grimme, *J. Chem. Phys.* **2006**, *124*, 034108.
- [46] S. Dohm, A. Hansen, M. Steinmetz, S. Grimme, M. P. Checinski, *J. Chem. Theory Comput.* **2018**, *14*, 2596–2608.
- [47] M. Bursch, A. Hansen, P. Pracht, J. T. Kohn, S. Grimme, *Phys. Chem. Chem. Phys.* **2021**, *23*, 287–299.

Manuscript received: December 30, 2020
Revised manuscript received: February 23, 2021
Accepted manuscript online: March 17, 2021
Version of record online: May 28, 2021